Analytical and Bioanalytical Chemistry (2019) 411:6255–6264
https://doi.org/10.1007/s00216-018-1515-7

PAPER IN FOREFRONT

Capillary zone electrophoresis coupled to drift tube ion mobility-mass spectrometry for the analysis of native and APTS-labeled *N*-glycans

Kevin Jooß[1,2] · Sven W. Meckelmann[3,4] · Julia Klein[3,4] · Oliver J. Schmitz[3,4] · Christian Neusüß[1]

Received: 24 August 2018 / Revised: 16 October 2018 / Accepted: 23 November 2018 / Published online: 10 December 2018

Abstract

Capillary zone electrophoresis (CZE) based on electrophoretic mobility in the liquid phase and ion mobility spectrometry (IMS) based on mobilities in the gas phase are both powerful techniques for the separation of complex samples. Protein glycosylation is one of the most common post-translational modifications associated with a wide range of biological functions and human diseases. Due to their high structural variability, the analysis of glycans still represents a challenging task. In this work, the first on-line coupling of CZE with drift tube ion mobility-mass spectrometry (DTIM-MS) has been perfomed to further improve separation capabilities for the analysis of native and 8-aminopyrene-1,3,6-trisulfonic acid (APTS)-labeled *N*-glycans. In this way, a complexity of glycan signals was revealed which could not be resolved by these techniques individually, shown for both native and APTS-labeled glycans. Each individual glycan signal separated in CZE exhibited an unexpectedly high number of peaks observed in the IMS dimension. This observation could potentially be explained by the presence of isomeric forms, including different linkages, and/or gas-phase conformers. In addition, the type of sialic acid attached to glycans has a significant impact on the obtained drift time profile. Furthermore, the application of α2-3 neuraminidase enabled the partial assignment of peaks in the arrival time distribution considering their sialic acid linkages (α2-3/α2-6). This work is a showcase for the high potential of CZE-DTIM-MS, which is expected to find various applications in the future.

Keywords Glycan analysis · CE-IM-MS · Isomer separation · Liquid- and gas-phase separation

Abbreviations

AGP	α-1-Acid glycoprotein
APTS	8-Aminopyrene-1,3,6-trisulfonic acid
ATD	Arrival time distribution
BGE	Background electrolyte
CE	Capillary electrophoresis
CZE	Capillary zone electrophoresis
DT	Drift time
DTIM-MS	Drift tube ion mobility-mass spectrometry
ESI	Electrospray ionization
FAIMS-MS	High-field asymmetric waveform ion mobility spectrometry mass spectrometry
HILIC	Hydrophilic interaction chromatography
IMS	Ion mobility spectrometry
mAb	Monoclonal antibody
MS	Mass spectrometry
NeuNAc	*N*-Acetylneuraminic acid
NeuNGc	*N*-Glycolylneuraminic acid

Published in the topical collection *Close-Up of Current Developments in Ion Mobility Spectrometry* with guest editor Gérard Hopfgartner.

Electronic supplementary material The online version of this article (https://doi.org/10.1007/s00216-018-1515-7) contains supplementary material, which is available to authorized users.

✉ Christian Neusüß
Christian.Neusuess@hs-aalen.de

[1] Faculty of Chemistry, Aalen University, 73430 Aalen, Germany

[2] Research Unit Analytical BioGeoChemistry, Helmholtz Zentrum München, Ingolstädter Landstr. 1, 85764 Neuherberg, Germany

[3] Applied Analytical Chemistry, University of Duisburg-Essen, Universitätsstr. 5, 45141 Essen, Germany

[4] Teaching and Research Center for Separation, University of Duisburg-Essen, Universitätsstr. 5, 45141 Essen, Germany

SA	Sialic acid
SL	Sheath liquid
TOF-MS	Time-of-flight mass spectrometry
TWIM-MS	Traveling wave ion mobility-mass spectrometry

Introduction

Glycosylation represents the most common post translational modification of proteins with an estimation that approximately 50% of all proteins are glycosylated in eukariotic systems [1]. A variety of biological functions have been associated with protein glycosylation including immune response, protein regulation/interactions, apoptosis, and recognition of signals on the cell surface [2]. Furthermore, glycans are known to be involved in the development and progression of human diseases, especially cancer, inflammantoy diseases, rheumatoid arthritis, and Alzheimers disease [3]. Increased insight in the molecular and structural characteristics of glycans in biological processess led to the development of biotherapeutics, e.g., monoclonal antibodies (mAbs), with specific glycoforms [4].

Glycoproteins synthesized in living cell systems usually comprise macro- and micro-heterogeneity based on the complexity of the involved glycosylation processes [5]. On the one hand, macro-heterogeneity is described by the variability of glycosylation sites and number of attached glycans. In general, glycosylation can occur on asparagine (*N*-glycans) or on serine/threonine (*O*-glycans) residues. On the other hand, micro-heterogeneity is related to the variety of different glycan structures that can occur. Furthermore, even for glycans with the same elemental composition, the micro-heterogeneity can be extensively complex due to stereoisomers of monomer units, several potential linkage sites, anomeric configurations of glycosidic bonds, and the occurrence of multiple branching patterns [6].

Thus, the characterization of glycosylation remains challenging usually requiring several orthogonal methods. Besides analyses on the intact glycoprotein and glycopeptide level, the detailed characterization of glycosylation based on released glycans represents an important analytical task. In order to determine three-dimensional structures of glycans, nuclear magnetic resonance spectroscopy and X-ray crystallography can be applied [7]. Still, these techniques require pure and highly concentrated samples.

Matrix-assisted laser desorption/ionization time-of-flight mass spectrometry (TOF-MS) can be applied for rapid profiling of released glycans. Thereby, glycans are usually permethylated to improve ionization efficiency and stabilize sialylated glycans in positive ionization mode [8]. For liquid chromatography–based and mass spectrometry (MS)–based characterization, released glycans are often labeled with a fluorescence tag, such as 2-aminobenzamide, using reductive amination [9]. Common chromatographic techniques for released glycan analysis include hydrophilic interaction chromatography (HILIC), reversed-phase liquid chromatography, anion exchange chromatography, and porous graphitized carbon chromatography [10].

Besides chromatographic approaches, electromigrative separation techniques represent efficient tools to separate glycan isomers in complex samples. In this regard, capillary sieving electrophoresis coupled to laser-induced fluorescence detection using 8-aminopyrene-1,3,6-trisulfonic acid (APTS) as fluorescence tag exhibits high selectivity/sensitivity and is commonly applied in pharmaceutical analysis [9]. However, due to the lack of available glycan standards and the incompatibily of the electrolyte system with electrospray ionization (ESI), the assignment of peaks, especially for new glycan structures, is difficult or even not possible. Thus, in recent years, we have introduced a capillary zone electrophoresis (CZE)-MS method based on an ε-aminocaproic acid background electrolyte (BGE) showing similar separation performance [11]. In addition, this method can be applied for native and APTS-labeled *N*-glycan analysis. Still, the glycan structure characterization remains challenging due to the isomeric and branched nature of glycans.

In recent years, ion mobility spectrometry (IMS) in combination with MS has gained importance. TOF-MS is usually selected as mass analyzer due to the well-fitting duty cycles (IMS: ms range; TOF-MS: μs range). Several different IMS technologies have been developed, which are discussed in detail elsewhere [12]. In general, ions are separated according to their charge, size, and shape while traversing through a cell, filled with neutral inert gas, and guided by an electric field. In this way, isomers can potentially be separated. IMS technology has been frequently applied for the analysis of glycans [13]. Despite the already promising results achieved, the separation efficiency of IMS needs to be improved, especially for larger complex type *N*-glycans.

On the one hand, the separation mechanism in CZE is based on the electrophoretic mobility in the liquid phase, which can be manipulated depending on the choice of BGE, additives, and coatings. On the other hand, IMS is associated with gas-phase mobilities and thus, different selectivities can be expected. Therefore, the combination of these two powerful techniques represents a promising approach to gain further separation performance, which was highlighted in a recent trend article [14]. Still, their orthogonality has not been carefully evaluated so far [15]. Capillary electrophoresis (CE) has been hyphenated with high-field asymmetric waveform ion mobility spectrometry mass spectrometry (FAIMS-MS) [16] and traveling wave ion mobility-mass spectrometry (TWIM-MS) [17, 18]. Yet, the focus of these works was to reduce the mass spectral noise (FAIMS-MS) or to obtain simultaneous information on the conformational distribution and activity of enzymes (TWIM-MS), and not to gain additional separation

performance. Preliminary attempts to perform CE-DTIM-MS have been carried out in the late 1980s by the Hill group [19]. However, spray instability was an issue and hindered its application at that time.

Here, the aforementioned CZE-MS method for glycan analysis was coupled to drift tube ion mobility-mass spectrometry (DTIM-MS). To the best of our knowledge, this is the first successful hyphenation of CZE to DTIM-MS technology to improve the performance of the separation. APTS-labeled *N*-glycans released from a model mAb were characterized. In addition, native complex type *N*-glycans released from fetuin and α-1-acid glycoprotein (AGP) were analyzed. Furthermore, native glycan samples were treated with α2-3 neuraminidase and reanalyzed and changes in the glycan profile were investigated.

Materials and methods

Materials

Ultrapure water (electrical resistivity > 18 MΩcm) from an UltraClear UV system (Siemens water technologies, Günzburg, Germany) was used to prepare all BGEs, samples, and rinsing solutions. Methanol (MS-grade), isopropyl alcohol (MS-grade), acetonitrile (MS-grade), sodium hydroxide (≥ 98%), ammonia solution (ROTIPURAN® 30% p.a.), ammonium hydrogen carbonate (≥ 99%, p.a.), and acetic acid (ROTIPURAN® 100%, p.a.) were obtained from Carl Roth (Karlsruhe, Germany). N-Glycosidase F (rec. *E. coli*), AGP (bovine serum 99%), and fetuin (fetal calf serum) were purchased from Sigma Aldrich (Steinheim, Germany). ε-Aminocaproic acid (pure) was obtained from Merck (Darmstadt, Germany). *N*-Glycans released from a monoclonal antibody were labeled with APTS based on the procedure in our previous work [11]. α2-3 Neuraminidase S from New England Biolabs (Frankfurt, Germany) was applied. Bare fused-silica capillaries (50 μm inner diameter, 363 μm outer diameter) were purchased from Polymicro Technologies (Phoenix, AZ, USA).

Deglycosylation of AGP and fetuin samples was performed with N-glycosidase F. Accordingly, 200 μg of protein was solved in 20 μL digestion buffer (25 mM ammonium hydrogen carbonate, pH = 8.2 adjusted with 30% ammonia). Subsequently, samples were transferred to safe-lock tubes containing 15 units of *N*-glycosidase F and incubated for 24 h at 37 °C. The reaction was stopped by heating the samples to 100 °C for 5 min. For the cleavage of α2-3-linked sialic acids (SA), 4 μL of α2-3 neuraminidase (1 mg/mL) was added and the samples were incubated for 3 h at 37 °C (pH 6 adjusted with acetic acid).

CZE-IM-MS

CZE

An Agilent 7100 CE System (Agilent Technologies, Waldbronn, Germany) was applied for CZE separation using bare fused-silica capillaries with an inner diameter of 50 μm and a length of 80.0 cm. The BGE consisted of 0.1 M ε-aminocaproic acid and 0.5 M ammonia solved in methanol/water 1:1 [11]. The capillaries were preconditioned once by rinsing (using approximately 1 bar) with methanol (5 min), water (5 min), 1.2 M hydrochloric acid (5 min), water (5 min), 1 M sodium hydroxide (20 min), water (5 min), and BGE (10 min). For long-term or overnight storage, the capillary was rinsed (using approximately 1 bar) with water and air for 5 min, respectively. Every morning, the capillary was preconditioned briefly (using approximately 1 bar) with 1.2 M hydrochloric acid (1.5 min), water (5 min), 0.1 M sodium hydroxide (10 min), water (5 min), and BGE (10 min). Samples were injected hydrodynamically (50 mbar, 18 s). A constant voltage of + 30 kV was applied during separation. Electropherograms were slightly smoothed using a Quartic/Quintic Savitsky-Golay algorithm.

ESI-DTIM-MS

An Agilent 6560 Ion Mobility Quadrupole Time-of-Flight Mass Spectrometer (Agilent Technologies, Waldbronn, Germany) was used. The CZE-ESI-IM-MS coupling was performed with a commercial triple-tube sheath liquid interface (Agilent Technologies, Waldbronn, Germany). Bare fused-silica capillaries were positioned in such a way that they stuck visibly outside of the sheath liquid sprayer needle (approximately 1/5 of the capillary diameter). Different sheath liquid (SL) compositions were tested: isopropyl alcohol/water 1:1, 3:7, 7:3; methanol/water 1:1; and acetonitrile/water 1:1. The SL was delivered at a flow rate of 4 μL/min by a syringe pump (Cole-Parmer®, IL, USA) equipped with a 5-mL syringe (5MDF-LL-GT, SGE Analytical Science, Melbourne, Australia). The Agilent Jetstream Source was operated in the negative mode under the following conditions: gas temperature 220 °C, drying gas 2 L/min N_2, sheath gas temperature 200 °C, sheath gas flow 5 L/min N_2, VCap 3500 V, nozzle voltage 2000 V, and fragmentor 400 V. DTIM-MS parameters were as follows: nitrogen (3.95 Torr) applied as drift gas, trap fill time 30 ms, trap release time 150 μs, and maximum drift time was 60 ms. The drift voltage was 18.5 V/cm (drift tube entrance 1700 V, drift tube exit 250 V, drift tube length 78.236 cm). Data processing was carried out by using Agilent MassHunter Qualitative Analysis Navigator (B.08.00) and IM-MS Browser (B.08.00). Identification of glycan species was based on their *m*/*z* value in combination

with the known literature [20]. All extracted ion electropherograms (EIEs) were extracted with $\Delta m = \pm 0.1$ Da.

Results and discussion

APTS-labeled glycans: mAb

Derivatization with APTS is a common labeling procedure for CZE characterization of *N*-glycans. Thus, as an initial test for the CZE-IM-MS setup, APTS-labeled *N*-glycans released from a model mAb were analyzed. To the best of our knowledge, the obtained results represent the first IMS data of *N*-glycans with this type of labeling. As expected, a typical CZE separation profile was obtained including the mAb-based glycans G0F, the isomers G1F′(1,3) and G1F(1,6), and G2F as shown in Fig. 1a [11]. Multiple deprotonated ionic species ($[M-2H]^{2-}$ and $[M-3H]^{3-}$) were detected with the negative charges located at the highly acidic APTS label (Fig. 1b).

Interestingly, each individual arrival time distribution (ATD) of the glycan signals resolved in the CZE exhibits multiple peaks. Two prominent peaks were observed for the $[M-3H]^{3-}$ species as displayed in Fig. 1c. The $[M-3H]^{3-}$ profiles of G0F, G1F′(1,3)/G1F(1,6), and G2F are quite similar. Still, with increasing molecular mass, the DT peaks are not only shifted to higher drift times, as expected, but also better resolved. In addition, a third, small signal is appearing at higher drift times in the G2F spectra, indicating the presence

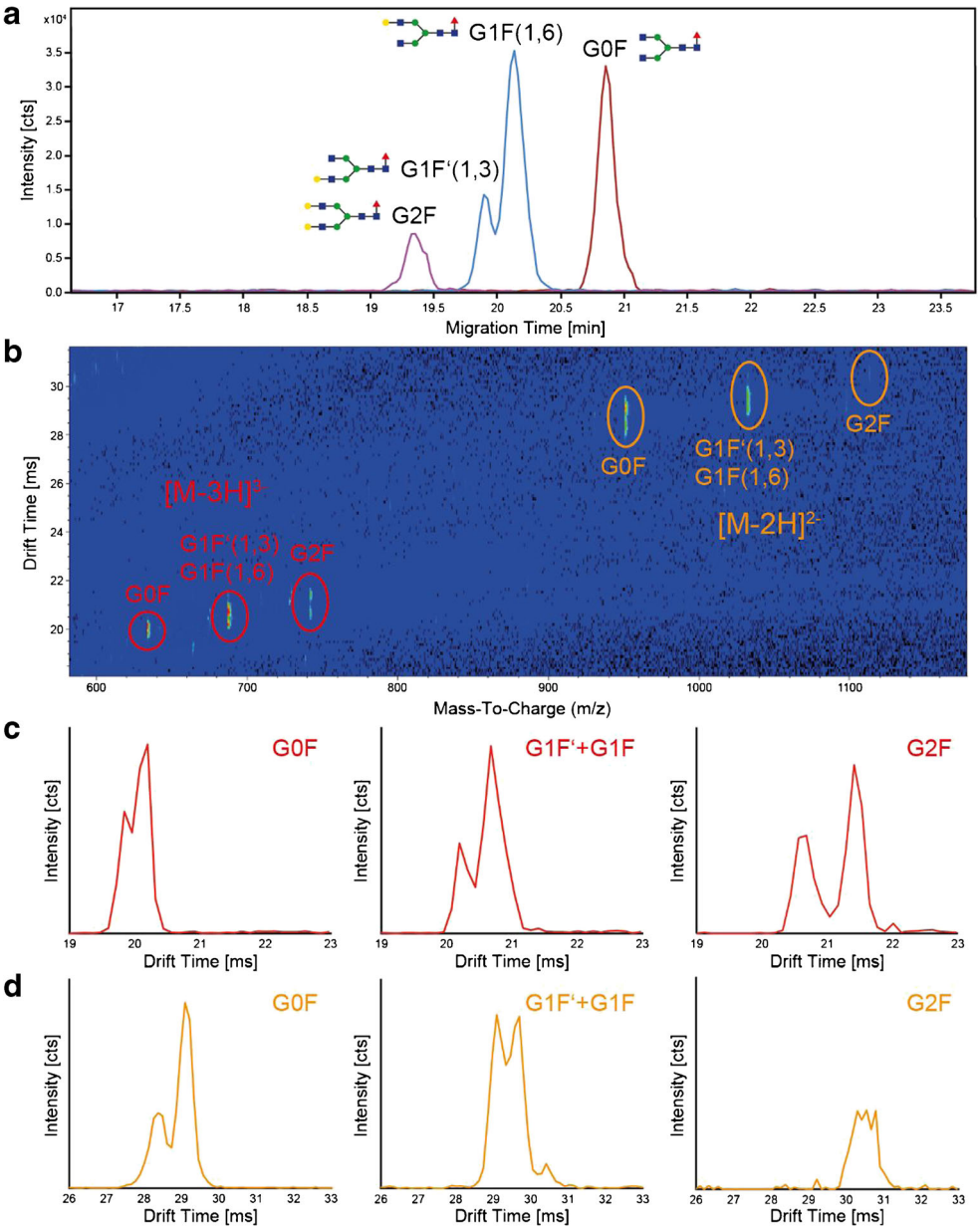

Fig. 1 CZE electropherogram of APTS-labeled *N*-glycans released from mAb1 including G0F (950.75, 633.50 *m/z*), G1F′(1,3) and G1F(1,6) (1031.77, 687.51 *m/z*), and G2F (1112.80, 741.53 *m/z*) (**a**). 2D IM-MS plot (19–21.2 min) (**b**): Heat map (*m/z* vs. DT) of triple- and double-charged ionic species highlighted in red and orange, respectively. ATDs of the glycans G0F (20.6–21.1 min), G1F′(1,3) + G1F(1,6) (19.7–20.5 min), and G2F (19.1–19.6 min) of the triply (**c**) and doubly (**d**) charged ions. Multiple peaks were observed in each ATD

of an ionic species with different mobility. Considering the ATD profiles of the $[M-2H]^{2-}$ signals, a change in the relative intensities in the pattern is more apparent than in the $[M-3H]^{3-}$ profiles (Fig. 1d). Still, the rather low signal intensity of G2F was not sufficient to allow an adequate comparison with the ATDs obtained from G0F and G1F′(1,3)/G1F(1,6).

The origin of the multiple peaks observed in the ATD space could not be unambiguously assigned, but could be explained by the presence of isomeric forms and/or conformers that do not interconvert on the time scale of the ion mobility separation. Though structural isomers of G0F and G2F are not described in the literature, an analogous ATD (double peak) was shown for G0F (pyridylamino labeled, $[M+2H]^{2+}$) analyzed by HILIC-IM-MS [21]. However, the authors did not elaborate on this observation. Nevertheless, we observed multiple signals in the ATD of all detected glycans. In recent years, there has been increased evidence that improved separation can be obtained in the IMS for certain isomeric glycans if deprotonated ionic species are analyzed, compared to other ionic species [22]. Still, gas-phase separation of glycan ions in IMS has been mainly focused on sodiated or other metal adducts. In addition, APTS-labeled glycans have not been analyzed by IMS so far. These circumstances complicate the comparison to other IMS related works.

Due to the preceding CZE separation, the isomers G1F′(1,3) and G1F(1,6) can be detected independently in the IMS. The distinct ATDs of the $[M-2H]^{2-}$ and $[M-3H]^{3-}$ ionic species of both G1F′(1,3) and G1F(1,6) are depicted in Fig. 2. It is apparent that the ATDs exhibit significant differences between G1F′(1,3) and G1F(1,6) for both charge states. For the triply charged species, G1F′(1,3) delivers one large peak with a slight shoulder on the lower side of the ATD. On the other hand, the ATD of G1F(1,6) indicates the presence of three different species. Considering the doubly charged ions, G1F′(1,3) exhibits the more complex profile with three prominent species, whereas G1F(1,6) shows only the two main ATD peaks. Summarized, without prior separation in the CZE dimension, the complexity of G1F′(1,3) and G1F(1,6) could not be resolved in the DTIM-MS and would result in overlaid ATDs. This observation highlights the important benefit of the hyphenation of CZE to DTIM-MS, since neither of these techniques would be able to resolve all the detected species individually.

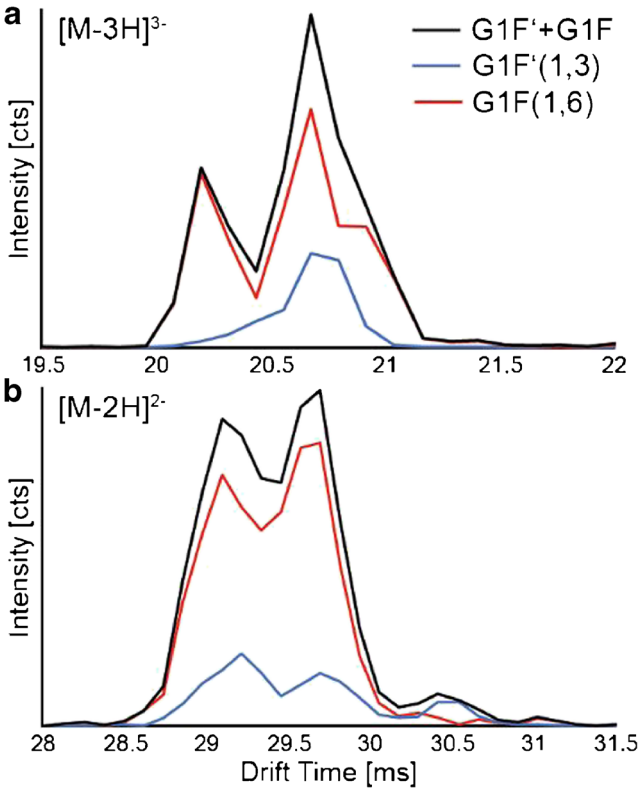

Fig. 2 ATDs of the triple-charged (**a**) and double-charged (**b**) ions originating from the mAb glycans G1F′(1,3) (blue, solid line) and G1F(1,6) (red, solid line) priorly separated by CZE. The MT region to extract the ATDs for G1F′(1,3) (19.74–19.89 ms) and G1F(1,6) (20.15–20.25 ms) was selected in certain distance from each other to minimize potential overlap of the ATDs. The combined information of G1F′(1,3) + G1F(1,6) (black, solid line) highlights that the ATDs of G1F′(1,3) and G1F(1,6) would overlap without prior CZE separation which would lead to substantial loss of information

Native glycans: AGP and fetuin

Besides APTS-labeled glycans, the CZE system can also be applied to native sialylated glycans. Therefore, native glycans released from fetuin and AGP were analyzed using the CZE-IM-MS setup. Example electropherograms of glycans released from AGP and fetuin are displayed in Fig. 3a, b. The major glycoforms detected for fetuin were di- and triantennary glycans with at least the same amount of *N*-acetylneuraminic acid (NeuNAc): 2Ant2NeuNAc, 3Ant3NeuNAc, and 3Ant4NeuNAc. On the other hand, AGP exhibits mostly diantennary carbohydrate chains with two to four sialyl residues: 2Ant2NeuNAc, 2Ant3NeuNAc, and 2Ant4NAc. This observation is in accordance with the literature [20]. ATDs of the major glycans for AGP and fetuin are shown in Fig. 3c–e and f–h, respectively. In comparison to the APTS-labeled mAb glycans, a similar or even higher complexity was obtained in the IMS dimension for the individual glycan peaks resolved by CZE. Similarly, Aizpurua-Olaizola et al. have shown more than one signal in the IMS profile of 2Ant1SA priorly separated by HILIC [14].

2Ant2NeuNAc is a major glycan of AGP and fetuin and, thus, allows the direct comparison of a glycan with the same saccharide composition from different protein sources (Fig. 3c, f). First, there are two ATD regions that are present in both proteins, which consist of at least two partly resolved peaks, respectively. However, in both ATD regions, the peaks detected at lower drift times are significantly higher for AGP in comparison to fetuin. Since both proteins were measured under the exact same conditions (instrument setup, BGE, SL composition, etc.), there is

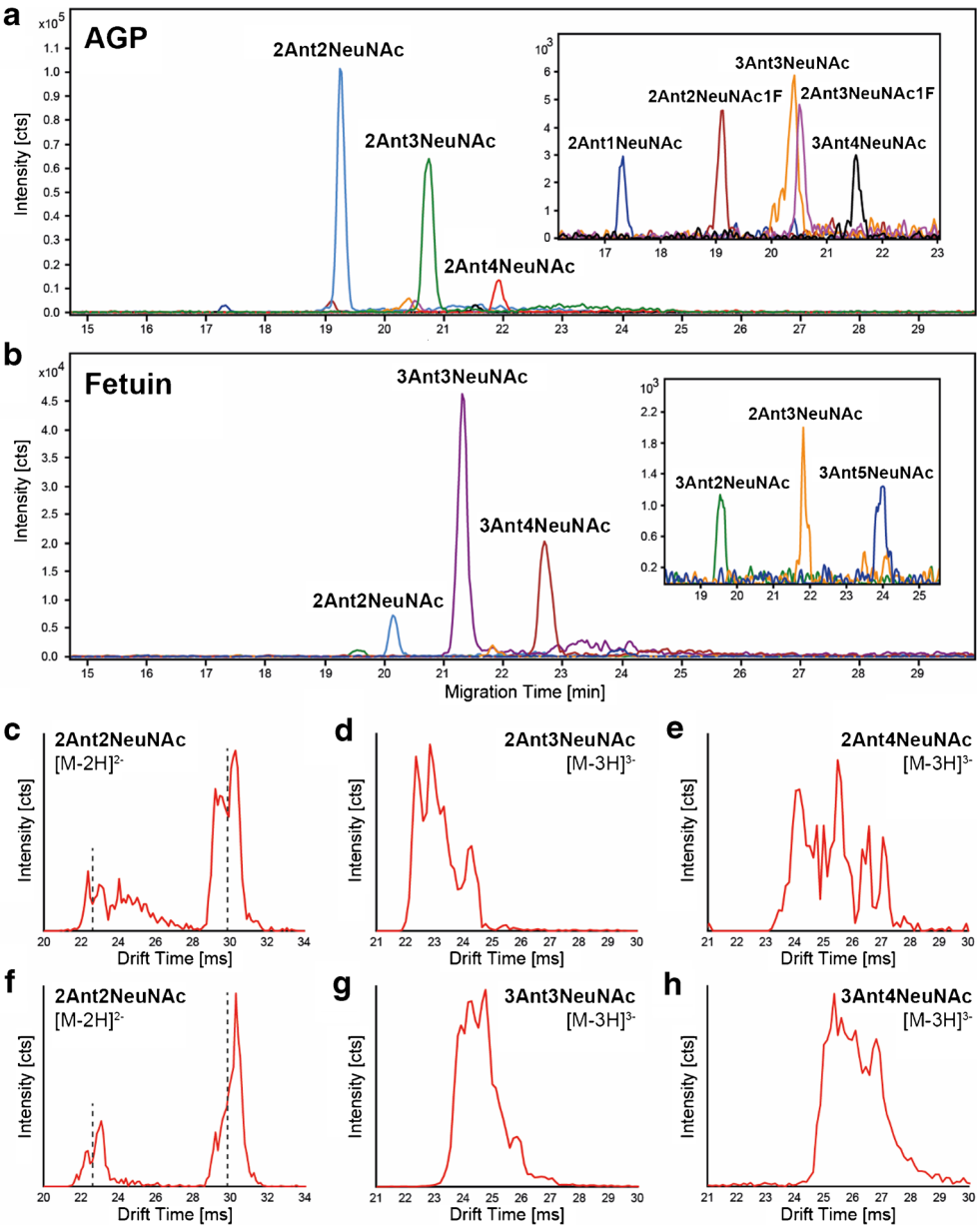

Fig. 3 CZE electropherograms of native sialylated *N*-glycans released from AGP (**a**) and fetuin (**b**): Major glycoforms detected include diantennary carbohydrate chains with two to four sialyl residues (AGP) and di- and triantennary glycans with at least the same amount of *N*-acetylneuraminic acid (fetuin). EICs of AGP are generated as a sum of both sialic acid types (NeuNAc and NeuNGc). Inserts show the lower abundant detected glycans, respectively. ATDs of AGP (**c**–**e**) and fetuin (**f**–**h**) glycans associated with the major peaks separated by CZE

evidence that some features do not correspond to gas-phase conformers, but rather linkage/structural isomers. In addition, AGP exhibits non-resolved signals between these two regions (Fig. 4b), which are barely visible for fetuin.

In contrast to the human form, bovine AGP exhibits glycans containing NeuNAc and/or *N*-glycolylneuraminic acid (NeuNGc) as SA residues increasing the overall complexity. To be more precise, each possible combination (relative amount) of both SA is present as exemplarily shown for the $[M-3H]^{3-}$ species of 2Ant3SA in Fig. 4a. The expected mass shift ($\Delta m/z = 5.33$) related to the exchange of NeuNAc to NeuNGc was observed in the mass spectra. It is also possible to partly separate the different SA types in the CZE dimension, which is exemplarily shown for 2Ant3SA in Fig. S1 (see Electronic Supplementary Material (ESM)). In the heat map (2D IM-MS plot, Fig. 4b), there appear to be minor differences between the ATDs in dependence of the type of SA residue which gets more evident by taking a closer look at the individual ATDs illustrated in Fig. 4c. The relative intensities of species change systematically with relative amount of NeuNGc. For example, the second observed peak is decreasing (black arrow) and the third one is increasing (blue arrow). An additional example is the ATDs for the $[M-2H]^{2-}$ species of 2Ant2SA (ESM Fig. S2). Similar changes of increasing and decreasing peaks were observed. However, in this regard, a clear statement is not possible due to the limited resolution.

An important parameter for the CZE-DTIM-MS system is the reproducibility of the obtained drift times and ATDs. In general,

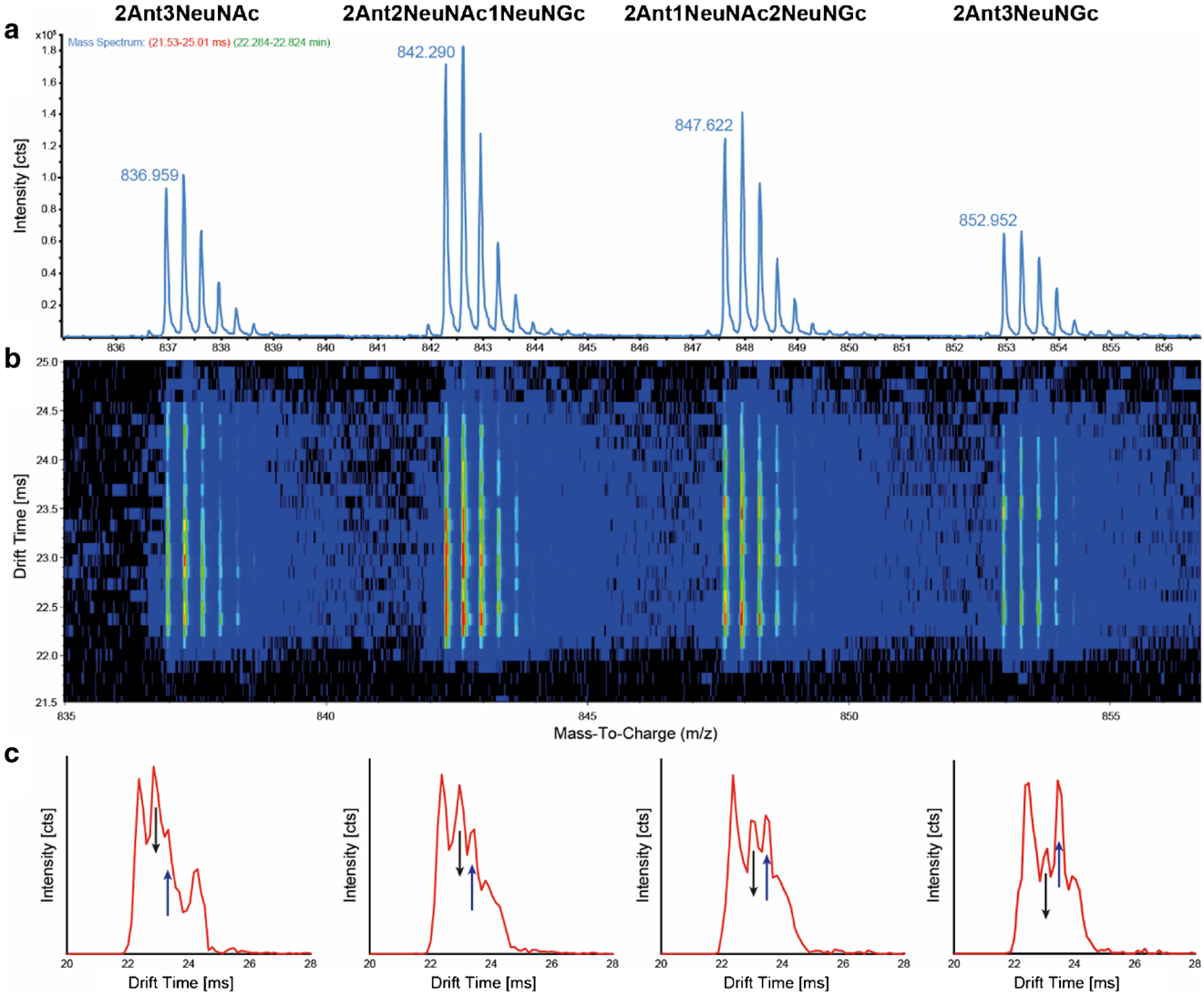

Fig. 4 Separation of 2Ant3SA species (AGP) with different sialic acids containing NeuNAc and/or NeuNGc. Mass spectra of $[M-3H]^{3-}$ ions (**a**) ranging from 2Ant3NeuNAc (836.959 *m*/*z*) to 2Ant3NeuNGc (852.952 *m*/*z*). Typical distances between sialic acid species were observed ($\Delta m/z = 5.33$). IMS heat map (**b**) associated with the mass spectra. Slight differences in the ATD are recognizable. Individual ATDs (**c**) of observed sialic acid species. Changes of relative intensities of signals in the obtained ATD observed in dependence of the type of sialic acid. Most distinct changes are indicated by arrows

the ATDs were reproducible for the entire measurement series. Exemplarily, the ATDs obtained for the glycans 2Ant1NeuNAc1NeuNGc and 2Ant1NeuNAc2NeuNGc of three measurements are shown in ESM Fig. S3. A mean RSD value of 0.20% was calculated for the drift times based on 12 peaks observed in the ATDs of 2Ant2SA (NeuNAc and NeuNGc variants) and 14 peaks observed in the ATDs of 2Ant3SA (NeuNAc and NeuGc variants) with $n_{total} = 148$. For the lower intense, noisier peaks, the RSD values for the drift times were typically around 0.5%. These values are in the range expected for this type of instrument [23].

In order to evaluate the influence of the sheath liquid on the ATDs, different SL combinations were tested analyzing *N*-glycans released from AGP: isopropyl alcohol/water 1:1, 3:7, 7:3; methanol/water 1:1; and acetonitrile/water 1:1. No significant changes in the ATDs could be observed (data not shown). In conclusion, the CE-IM-MS system seems to be not depending on the SL applied including the nature and relative amount of organic solvent. Thus, SL compositions can be adapted independently from the IMS dimension, e.g., optimizing ionization efficiency.

To further elucidate the characteristics of the multiple peaks observed in the ATDs, AGP and fetuin samples were treated with α2-3 neuraminidase. In this way, sialic acids exhibiting a α2-3 linkage to galactose are specifically cleaved and α2-6 linkages remain intact. The respective electropherograms of AGP and fetuin can be found in ESM Fig. S4. Interestingly, up to three peaks—corresponding to a single *m*/*z* value—are resolved by CZE as exemplarily depicted for 2Ant2SA released from AGP in Fig. 5a. Since liquid-phase conformers are

typically not separated by CZE, it can be assumed that the species resolved are isomers. These glycan structures should only contain α2-6 linkages after α2-3 neuraminidases treatment. Thus, the separation in CZE is not related with sialic acid linkages, as commonly observed by porous graphitized carbon chromatography, but can potentially be explained by differences in other linkages such as Gal1-3GlcNAc/Gal1-4GlcNAc in the glycan branches as detected by nuclear magnetic resonance spectroscopy [24]. The individual ATDs of the 2Ant2SA signals resolved in CZE are shown in Fig. 5b. The first and the second CZE peaks showed a similar profile in the ATD. The complexity increased towards the third CZE peak, which exemplarily exhibited a high intense additional feature in the higher ATD region ($t_d = 29.2$ ms). The separation of glycan species in CZE in combination with the further gained resolution in the DTIM-MS indicates again the potential of the hyphenation of these two powerful analytical techniques. By comparing the ATDs before and after α2-3 neuraminidase treatment, it is possible to partly assign signals observed in the ATD. This is especially the case for 2Ant2NeuNAc released from fetuin as illustrated in Fig. 6. In contrast to AGP, fetuin did not exhibit significant amounts of diantennary glycans with more than two sialic acid attached. Thus, only a loss of certain species in the ATD can be expected. The decrease of **(2)** and **(4)** is evidence that these regions of the ATD originally contained partly glycans with at least one α2-3-linked NeuNAc. On the other hand, the signals **(1)** and **(3)** in the ATD apparently consist of glycans only containing α2-6-linked SA. Again, the presence of multiple peaks only constituted of α2-6-linked SA could potentially be explained by differences in other linkages such as Gal1-3GlcNAc/Gal1-4GlcNAc in the glycan branches.

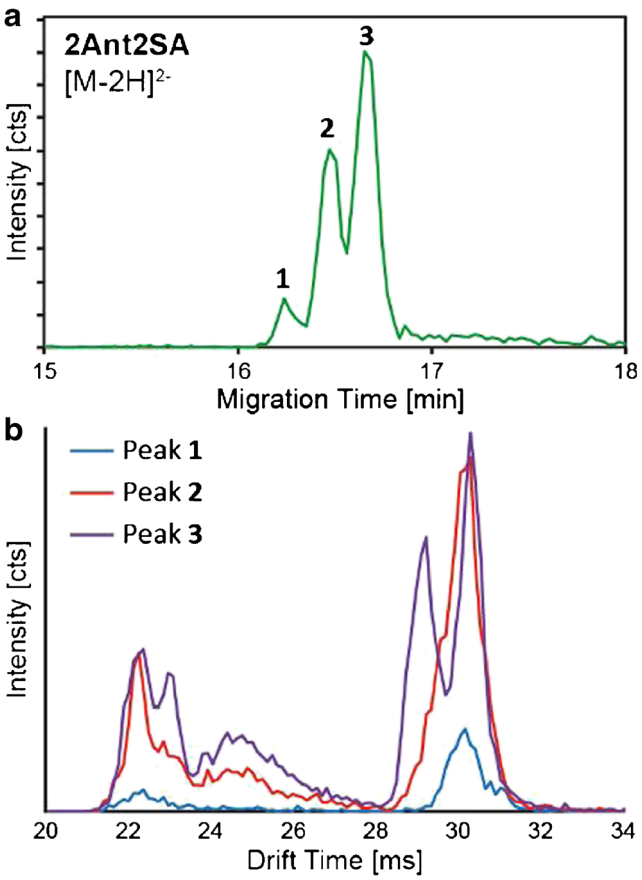

Fig. 5 CZE electropherogram of 2Ant2SA released from AGP and treated with α2-3 neuraminidase (**a**). EICs were generated using the combined information of all sialic acid variants related to 2Ant2SA (NeuNAc + NeuNGc). Three distinct peaks could be separated by CZE. Individual ATDs of CZE peaks 1–3 (**b**). Differences in the ATDs were observed

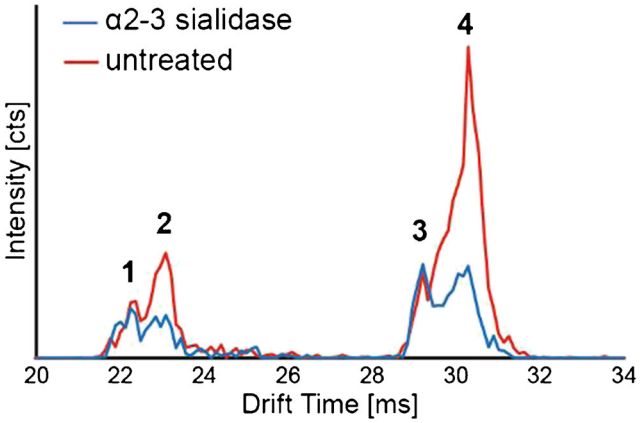

Fig. 6 ATD of 2Ant2NeuNAc ($[M-2H]^{2-}$ species) released from fetuin before (red, solid line) and after (blue, solid line) α2-3 neuraminidase treatment, divided into four regions (1–4). Decrease of the peaks (2) and (4) observed, whereas (1) and (3) remain similar in intensity

Conclusion

The combination of CZE and DTIM-MS technology was successfully applied for the separation and characterization of native and APTS-labeled *N*-glycans released from different protein sources. In general, each individual glycan signal resolved in CZE exhibited multiple peaks in the ATD. This observation could be explained by the presence of isomeric forms, including different linkages, and/or gas-phase conformers which do not interconvert on the time scale of the ion mobility separation. Without prior separation in the CZE dimension, the complexity of some *N*-glycans could not be resolved by DTIM-MS alone and would unavoidably lead to overlaid ATDs. This could be shown exemplarily for both APTS-labeled G1F′(1,3)/G1F(1,6) isomers (mAb) and native 2Ant2SA species after α2-3 neuraminidase treatment (bovine AGP). Since neither CZE nor

DTIM-MS would be able to resolve all the detected species individually, these examples highlight the advantages achieved by the combination of these powerful analytical techniques. For native 2Ant2NeuNAc, differences in the ATD profile were observed depending on the proteins (AGP or fetuin) it originated from, measured under the same conditions. This is evidence that some features do not correspond to gas-phase conformers, but rather to linkage/structural isomers. In addition, it could be shown that the nature and type of SL did not noticeably affect the obtained ATDs. Thus, SL compositions can be optimized regarding ionization efficiency independently from the DTIM-MS dimension. Bovine AGP exhibits a unique feature by possessing two types of SA, NeuNAc and NeuNGc. Besides the partial separation in the CZE dimension, systematic differences in the relative intensities of the ATD were observed in dependence of the type of sialic acid. Furthermore, the use of α2-3 neuraminidase enables a partial assignment of peaks observed in the DTIM-MS spectra in regard to sialic acid linkages. Summarized, the combination of CZE and DTIM-MS technology displays a high potential and is expected to find various applications in the future.

Compliance with ethical standards

Conflict of interest The authors declare that they have no conflict of interest.

Publisher's Note Springer Nature remains neutral with regard to jurisdictional claims in published maps and institutional affiliations.

References

1. Williams JP, Grabenauer M, Holland RJ, Carpenter CJ, Wormald MR, Giles K, et al. Characterization of simple isomeric oligosaccharides and the rapid separation of glycan mixtures by ion mobility mass spectrometry. Int J Mass Spectrom. 2010;298(1–3):119–27.
2. Rudd PM. Glycosylation and the immune system. Science. 2001;291(5512):2370–6.
3. Montreuil J, Vliegenthart JFG, Glycoproteins SH. New comprehensive biochemistry, vol. 29a. Amsterdam: Elsevier; 1995.
4. Dalziel M, Crispin M, Scanlan CN, Zitzmann N, Dwek RA. Emerging principles for the therapeutic exploitation of glycosylation. Science. 2014;343(6166):1235681.
5. Zhang L, Luo S, Zhang B. Glycan analysis of therapeutic glycoproteins. MAbs. 2016;8(2):205–15.
6. Dwek RA. Glycobiology: toward understanding the function of sugars. Chem Rev. 1996;96(2):683–720.
7. Wormald MR, Petrescu AJ, Pao Y-L, Glithero A, Elliott T, Dwek RA. Conformational studies of oligosaccharides and glycopeptides: complementarity of NMR, X-ray crystallography, and molecular modelling. Chem Rev. 2002;102(2):371–86.
8. Sanchez-De Melo I, Grassi P, Ochoa F, Bolivar J, García-Cózar FJ, Durán-Ruiz MC. N-glycosylation profile analysis of trastuzumab biosimilar candidates by normal phase liquid chromatography and MALDI-TOF MS approaches. J Proteome. 2015;127:225–33.
9. Ruhaak LR, Zauner G, Huhn C, Bruggink C, Deelder AM, Wuhrer M. Glycan labeling strategies and their use in identification and quantification. Anal Bioanal Chem. 2010;397(8):3457–81.
10. Melmer M, Stangler T, Premstaller A, Lindner W. Comparison of hydrophilic-interaction, reversed-phase and porous graphitic carbon chromatography for glycan analysis. J Chromatogr A. 2011;1218(1):118–23.
11. Bunz S-C, Cutillo F, Neusüß C. Analysis of native and APTS-labeled N-glycans by capillary electrophoresis/time-of-flight mass spectrometry. Anal Bioanal Chem. 2013;405(25):8277–84.
12. Kanu AB, Dwivedi P, Tam M, Matz L, Hill HH. Ion mobility-mass spectrometry. J Mass Spectrom. 2008;43(1):1–22.
13. Hofmann J, Pagel K. Glycan analysis by ion mobility-mass spectrometry. Angew Chem Int Ed. 2017;56(29):8342–9.
14. Aizpurua-Olaizola O, Sastre Toraño J, Falcon-Perez JM, Williams C, Reichardt N, Boons G-J. Mass spectrometry for glycan biomarker discovery. TrAC Trends Anal Chem. 2018;100:7–14.
15. Zheng X, Wojcik R, Zhang X, Ibrahim YM, Burnum-Johnson KE, Orton DJ, et al. Coupling front-end separations, ion mobility spectrometry, and mass spectrometry for enhanced multidimensional biological and environmental analyses. Ann Rev Anal Chem. 2017;10(1):71–92.
16. Li J, Purves RW, Richards JC. Coupling capillary electrophoresis and high-field asymmetric waveform ion mobility spectrometry mass spectrometry for the analysis of complex lipopolysaccharides. Anal Chem. 2004;76(16):4676–83.
17. Mironov GG, Okhonin V, Khan N, Clouthier CM, Berezovski MV. Conformational dynamics of DNA G-quadruplex in solution studied by kinetic capillary electrophoresis coupled on-line with mass spectrometry. Chem Open. 2014;3(2):58–64.
18. Mironov GG, Clouthier CM, Akbar A, Keillor JW, Berezovski MV. Simultaneous analysis of enzyme structure and activity by kinetic capillary electrophoresis–MS. Nat Chem Biol. 2016;12(11):918–22.
19. Hallen RW, Shumate CB, Siems WF, Tsuda T, Hill HH. Preliminary investigation of ion mobility spectrometry after capillary electrophoretic introduction. J Chromatogr. 1989;480:233–45.
20. Nakano M. Detailed structural features of glycan chains derived from 1-acid glycoproteins of several different animals: the presence of hypersialylated, O-acetylated sialic acids but not disialyl residues. Glycobiology. 2004;14(5):431–41.
21. Yamaguchi Y, Nishima W, Re S, Sugita Y. Confident identification of isomeric N-glycan structures by combined ion mobility mass spectrometry and hydrophilic interaction liquid chromatography. Rapid Commun Mass Spectrom. 2012;26(24):2877–84.
22. Struwe WB, Baldauf C, Hofmann J, Rudd PM, Pagel K. Ion mobility separation of deprotonated oligosaccharide isomers – evidence for gas-phase charge migration. Chem Commun. 2016;52(83):12353–6.
23. Stow SM, Causon TJ, Zheng X, Kurulugama RT, Mairinger T, May JC, et al. An interlaboratory evaluation of drift tube ion mobility-mass spectrometry collision cross section measurements. Anal Chem. 2017;89(17):9048–55.
24. Cumming DA, Hellerqvist CG, Harris-Brandts M, Michnick SW, Carver JP, Bendiak B. Structures of asparagine-linked oligosaccharides of the glycoprotein fetuin having sialic acid linked to N-acetylglucosamine. Biochemistry. 1989;28:6500–12.

Kevin Jooß is currently a Ph.D. student at Aalen University and the Helmholtz Zentrum München. He has been working on the analysis of small molecule drugs, complex proteins, and N-glycans applying capillary zone electrophoresis mass spectrometry. His Ph.D. project is related to the development and application of two-dimensional (electromigrative) separation techniques coupled to mass spectrometry.

Sven W. Meckelmann is Senior Scientist at the University of Duisburg-Essen in the Department of Applied Analytical Chemistry. His research interests include the development and application of new methods for the identification and quantification of lipids and metabolites in biological samples.

Julia Klein is currently a Ph.D. student in the working group of Professor Oliver J. Schmitz for Applied Analytical Chemistry at the University of Duisburg-Essen, Germany. Her research focusses on the analysis of complex samples using liquid chromatography coupled to ion mobility and high-resolution mass spectrometry.

Oliver J. Schmitz cofounded the company iGenTraX UG which develops new ion sources and units to couple separation techniques with mass spectrometers. Since 2012, he has been Full Professor at the University of Duisburg-Essen and is Chair of the Institute of Applied Analytical Chemistry. In 2018, he founded the Teaching and Research Center for Separation (TRC) at the University of Duisburg-Essen, which belongs to Agilent's global network of world-class Centers of Excellence. He is the author/co-author of one textbook and 9 book chapters, 81 papers published in peer-reviewed journals, more than 130 lectures, and 4 patents.

Christian Neusüß is Full Professor at the Faculty of Chemistry at Aalen University. His research interests include sophisticated separation techniques coupled to (high-resolution) mass spectrometry with a focus on CE-MS. His latest research focus is set on the development of two-dimensional electromigrative separation techniques coupled to mass spectrometry. He is the author/co-author of about 100 peer-reviewed publications and several patents and book chapters as well as numerous lectures at scientific conferences.